Technical Notes

Hemodynamic assessment of partial mechanical circulatory support: data derived from computed tomography angiographic images and computational fluid dynamics

Christof Karmonik[1], Sasan Partovi[2], Fabian Rengier[3,4], Hagen Meredig[3], Mina Berty Farag[5], Matthias Müller-Eschner[3,4], Rawa Arif[5], Aron-Frederik Popov[6], Hans-Ulrich Kauczor[3], Matthias Karck[5], Arjang Ruhparwar[5]

[1]Magnetic Resonance Imaging Core, Houston Methodist Research Institute, Houston, Texas, USA; [2]Department of Radiology, University Hospitals Case Medical Center, Case Western Reserve University, Cleveland, Ohio, USA; [3]Department of Diagnostic and Interventional Radiology, University Hospital Heidelberg, Heidelberg, Germany; [4]Department of Radiology E010, German Cancer Research Center (DKFZ), Heidelberg, Germany; [5]Department of Cardiac Surgery, University Hospital Heidelberg, Heidelberg, Germany; [6]Department of Cardiothoracic Transplantation and Mechanical Support, Royal Brompton and Harefield NHS Trust, Harefield Hospital, London, UK

Correspondence to: Sasan Partovi, MD. Department of Radiology, University Hospitals Case Medical Center, Case Western Reserve University, 11100 Euclid Ave, Cleveland, Ohio 44106, USA. Email: sasan.partovi@case.edu or sasan.partovi@uhhospitals.org.

Abstract: Partial mechanical circulatory support represents a new concept for the treatment of advanced heart failure. The Circulite Synergy Micro Pump®, where the inflow cannula is connected to the left atrium and the outflow cannula to the right subclavian artery, was one of the first devices to introduce this concept to the clinic. Using computational fluid dynamics (CFD) simulations, hemodynamics in the aortic tree was visualized and quantified from computed tomography angiographic (CTA) images in two patients. A realistic computational model was created by integrating flow information from the native heart and from the Circulite device. Diastolic flow augmentation in the descending aorta but competing/antagonizing flow patterns in the proximal innominate artery was observed. Velocity time curves in the ascending aorta correlated well with those in the left common carotid, the left subclavian and the descending aorta but poorly with the one in the innominate. Our results demonstrate that CFD may be useful in providing a better understanding of the main flow patterns in mechanical circulatory support devices.

Keywords: Heart failure; partial mechanical circulatory support; computational fluid dynamics (CFD); flow

Submitted Jan 10, 2015. Accepted for publication Feb 09, 2015.
doi: 10.3978/j.issn.2223-3652.2015.03.03
View this article at: http://dx.doi.org/10.3978/j.issn.2223-3652.2015.03.03

Introduction

Left ventricular assist devices (LVAD) with full mechanical support and left-ventricular unloading are limited to end-stage heart-failure patients. In contrast, partial mechanical circulatory support devices are intended for patients at an earlier stage of heart failure. The Circulite Synergy Micro-pump was the first of such a device (1-3) that has been applied clinically and has been demonstrated to be associated with significantly improved hemodynamics in a study of 27 New York Heart Association class IIIB and early class IV patients (2).

Conceptually, the support flow created by the Circulite Synergy Micro-pump with its inflow graft connected to the left atrium travels from the anastomosis site of the outflow graft at the right subclavian artery through the innominate artery (flow reversal) to the aorta. Alterations in hemodynamics with this new concept are not well understood. Direct measurements are only available from Doppler ultrasound techniques as the device itself is a contraindication to other methods such as phase contrast magnetic resonance imaging. Non-invasive Doppler techniques are limited to selected arterial segments and

a complete three-dimensional picture of the entire flow field during the cardiac cycle is not easily obtained. An alternative to direct measurements is the indirect calculation of hemodynamics using computational fluid dynamics (CFD). In this approach, the geometry of the arterial tree and the inflow and outflow conditions of the arterial segment of interest are used to solve the Navier Stokes partial differential equation which yields a complete three-dimensional description of the blood flow velocity for the entire cardiac cycle.

Here, we demonstrate the use of CFD based on computed tomography angiographic (CTA) images and Doppler ultrasound measurements obtained from two patients. We aimed to demonstrate the interaction between flow created by the device and the pulsatile native cardiac outflow at different time points in the cardiac cycle.

Materials and methods

Patient information

Permission of the Internal Review Board was obtained for this retrospective study. Two female patients, both 63 years old, with ischemic cardiomyopathy post Circulite Synergy Micro-pump implantation underwent a CTA examination using a SOMATOM Definition Flash CT scanner (Siemens, Erlangen, Germany) and retrospective ECG-gating within 2 months after device implantation. The dose length products of the two CTA studies were 1,147 and 1,943 mGycm, respectively.

Computational fluid dynamics (CFD) technique

The lumen of the thoracic aorta, the origins of the supra-aortic vessels and the right subclavian artery including the outflow anastomosis site were manually segmented. From this segmentation, a 3D surface reconstruction of the luminal boundary was created (Paraview, Kitware Inc.). The native cardiac outflow velocity waveform was reconstructed from measurements obtained with transthoracic Doppler (TTD) echocardiography and used as inflow waveform in the CFD simulations as was the (constant) outflow velocity of the Circulite Synergy Micro-pump (*Figure 1* and *Table 1*). The 3D surface reconstruction of the segmented lumen was imported into Star-CCM+ (version 8.02.008) and computational polyhedral meshes were created (case 1: 121,740 elements; case 2: 112,897 elements). Blood was modeled as a Newtonian fluid with a constant density of 1,050 kg/m^3 and a constant viscosity of 0.004 Pa·s. A laminar flow model was assumed (no inclusion of turbulence effects). To allow for the decay of initial transients in the computational simulation, three cardiac cycles were and results are reported from the third cardiac cycle with a method described previously (4).

Post-processing of simulation results

Total velocities, velocities in the inferior-superior direction and pressures were temporally averaged in the proximal innominate artery, the left common carotid artery and the left subclavian artery. Velocity time curves in these arteries were compared with the one of the ascending aorta using the Pearson correlation coefficient as means to reveal modifications of the hemodynamics. Pseudo-color representations of velocity magnitudes, pressures and wall shear stresses (WSS) during systole and diastole were created to illustrate overall hemodynamics in the computational model.

Results

Case 1

Pressures in the distal subclavian artery immediately proximal to the anastomosis site exhibited elevated pressures during the entire cardiac cycle compared to the remainder of the arteries, where high pressures were only observed during systole (*Figure 1A*). During diastole, prominent retrograde flow from the outflow graft anastomosis site entering the aorta was observed (*Figure 1B*). This flow was reversed during peak systole in the proximal innominate and subclavian arteries due to increased native cardiac output, causing a "collision" of both flows, leading to unordered and stagnant flow. In addition, a region of recirculating or slow flow formed in the proximal subclavian artery at this time, which traveled more proximal during beginning and end systole. For case 1, the retrograde average velocity in the innominate was 0.03 m/s during diastole which, was reversed during systole with an average of 0.08 m/s. The average total velocity in the left innominate was considerably lower than the velocities in the other two supra-aortic vessels but pressures where the highest of all three (*Figure 2*). A low correlation of 0.31 between the velocity time curve in the ascending aorta and the innominate artery further points to disturbed flow in this artery.

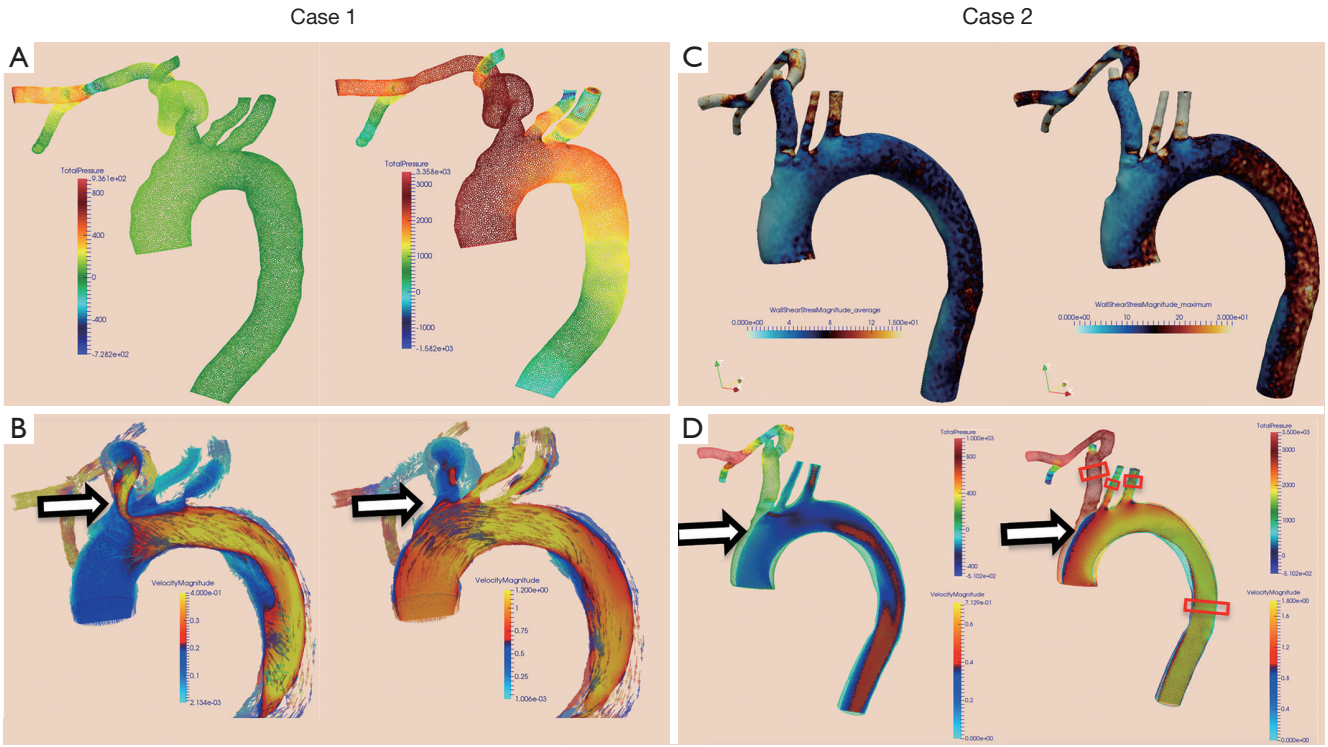

Figure 1 (A) Pressure distribution on the wall of the computational model for case 1 during diastole (left) and systole (right). While elevated pressures in systole exist in the ascending aorta and the innominate, these are only found at the anastomosis site during diastole; (B) flow patterns for case 1 (visualized by the velocity magnitude) demonstrate a change in the overall flow pattern, which is dominated during diastole by the Circulite device and during systole by the native flow from the heart; (C) WSS maximum and average during the cardiac cycle both exhibit a minimum at the anterior wall of the ascending aorta but also a maximum at the anastomosis site; (D) as for case 1, also the flow patterns for case 2 (visualized by the velocity magnitude) demonstrate a change in the overall flow pattern, which is dominated during diastole by the Circulite device and during systole by the native flow from the heart. Red boxes mark the regions where velocities and pressures were quantified. WSS, wall shear stresses.

Table 1 Hemodynamics data for both cases

Items	Case 1	Case 2
Outflow graft (m/s)	0.843	0.929
RR interval (msec)	500	900
EF (%)	21	17
SV (mL)	65.5	51.1
EDV (mL)	311.4	306.9
ESV (mL)	245.9	255.8
Cardiac outflow (L/min)	7.4	2.3

EF, ejection fraction; SV, stroke volume; EDV, end diastolic volume; ESV, end systolic volume.

The blood flow of this case is illustrated in the *Figures 3* and *4*.

Case 2

A similar flow pattern was observed for case 2 as described for case 1 with a reversal of retrograde average velocity from 0.18 m/s during diastole and of 0.12 at systole (*Figure 1D*). Average and maximum WSS values exhibited a maximum at the anastomosis site but also a minimum on the anterior wall of the ascending aorta (*Figure 1C*). Also for this case, average total velocity in the innominate artery was

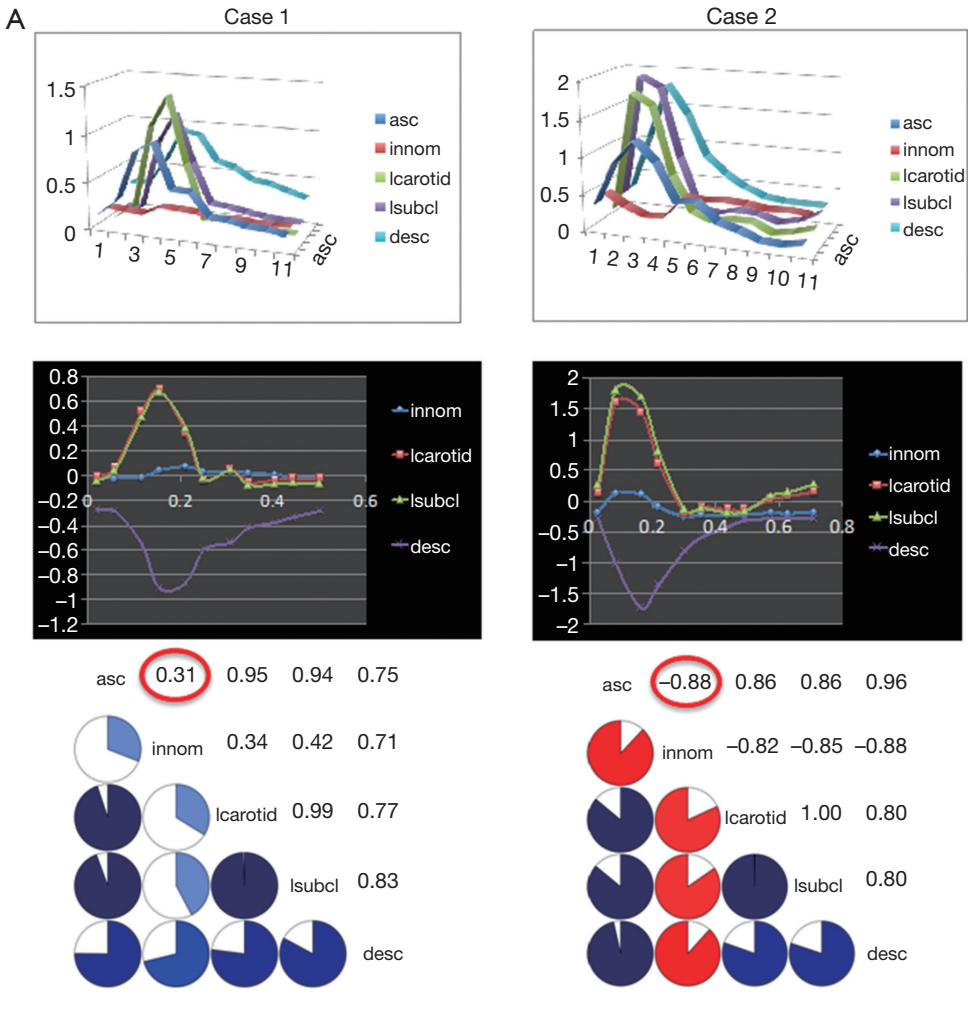

B

Case 1	velocity	IS velocity	pressure
asc	0.397		
innom	0.192	0.015	479
lcarotid	0.335	0.136	371
lsubcl	0.324	0.119	297
desc	0.515	−0.496	309

Case 2	velocity	IS velocity	pressure
asc	0.501		
innom	0.398	−0.142	853
lcarotid	0.464	0.317	552
lsubcl	0.553	0.402	624
desc	0.669	−0.672	593

Figure 2 (A) Top panel: velocity time curves in the ascending aorta (asc), the innominate artery (innom), the left carotid artery (lcarotid), the left subclavian artery (lsubcl) and the descending aorta (desc) for both cases. The deviation of shape for the innominate artery can be appreciated for both cases, likely related to the described hemodynamics. Middle panel: velocity time curves for flow in inferior-superior direction. Flow reversal during cardiac cycle in the innominate is clearly visible pointing to competing effects of flow created by the Circulate device and by the native heart. Lower panel: the upper triangular matrix displays the correlation coefficients between the velocity time curves shown in A while the lower triangular matrix graphically visualizes these correlation coefficients (blue: positive, red: negative). Low positive correlation for case 1 and strong negative correlation for case 2 quantifies the difference in shapes shown in the upper panel; (B) average values of velocities, velocities in inferior-superior direction (IS velocity) and pressure for both cases.

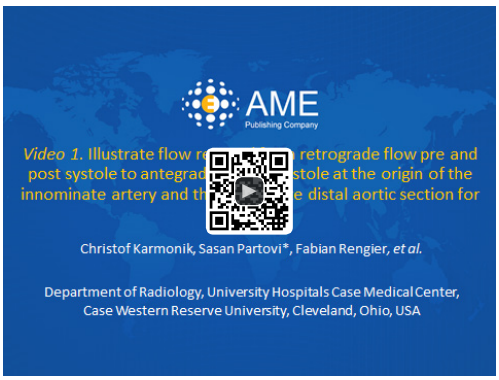

Figure 3 Illustrates flow reversal from retrograde flow pre and post systole to antegrade flow at systole at the origin of the innominate artery and the immediate distal aortic section for case 1 (5). Higher flow velocities are indicated by yellow, orange and red colors. A region of slow and stagnant flow can be appreciated in the anterior ascending aorta during systole. Also during systole, the lowest blood flow velocities can be found at this location. These observed alterations in hemodynamics are a direct consequence of competing flows from the partial support device and native cardiac output.
Available online: http://www.asvide.com/articles/470

Figure 4 Shows the entire model in similar fashion as supplement #1 (6). Inflow from the partial support device is indicated by high velocities (yellow and red colors) on the left. Interacting flows of opposite direction meet at the proximal section of the innominate artery resulting in a 'traveling' band of slow velocities (dark blue region). Flow patterns are complex pre and post systole and deviate considerably from the pattern at systole where native flow from the heart dominates.
Available online: http://www.asvide.com/articles/471

lowest for the innominate and flow direction on average was actually retrograde (*Figure 2*).

Discussion

To access efficacy of new partial mechanical circulatory support devices, a better understanding of the induced flow alterations is warranted. Direct measurements *in vivo* are difficult to obtain for the entire artery tree. As an alternative, we have demonstrated that CFD in combination with clinical CTA images together with patient-specific inflow boundary conditions, is capable of reproducing flow feature in the aorta and adjacent arteries. While blood velocity was increased in the aorta distal to the origin of the innominate artery during diastole, flow during systole was not affected as the Circulite device and the native cardiac output worked against each other thereby creating an area of recirculating flow in the distal innominate artery partially extending into the subclavian artery. Clinical studies evaluating the effectiveness of the Circulite Synergy Micro-pump have reported encouraging results, demonstrating that the device improved hemodynamics in heart failure patients of class IIIB and IV and appeared to interrupt and partially reverse the progressive hemodynamic deterioration typical of end-stage heart failure (2). In a study of 54 chronic heart failure patients, older patients (≥70 years) implanted with Synergy had smaller body sizes and worse renal function than younger patients. Both groups experienced similar hemodynamic benefits and functional improvements, though peak VO_2 was less improved in the elderly (3).

Our results demonstrate increased support of aortic flow during most of the cardiac cycle, but ineffectiveness of the device during peak systole. As a consequence of the flow reversal in the innominate artery, a region of low and oscillating wall shear stress WSS is created. This particular hemodynamic condition has previously been identified to be promote atherosclerosis by inducing endothelial cell apoptosis via a mechanism that involves the induction of GATA4, FZD5 and BMP2; molecules that have a well-defined role in embryonic development (7). A recent microRNA study reported alterations in miR-regulated differential gene expressions with varying hemodynamic forces. Several microRNAs were identified mediating a protective role with high WSS and expression of miR-21, miR-92a, and miR-663 activated with low WSS resulted in a pathological EC phenotype (8). A synchronization of partial mechanical support devices to the cardiac cycle of the individual may avoid this potential adverse hemodynamic condition and potentially improve outcome.

As with any model, our CFD results present a simplification of reality in which only the most pertinent features were considered. Aortic wall motion effects were not included nor were fluid structure interactions of the aortic wall with surrounding parenchyma. Consequently, our results have to be considered to reproduce major flow patterns, which may be refined by including the features discussed above. Nevertheless, they help to understand the general concept of the altered hemodynamics: antagonistic flows between the heart and the supporting device during systole interfere in a destructive pattern. As no device-specific assumptions were included in the CFD simulation, similar flow patterns may be anticipated for other such kind of devices unless alternative algorithms of pump activity are implemented.

In contrast to patients with conventional continuous flow LVADs, patients with partial mechanical circulatory support still have a considerable output of the native heart and antagonistic flows between the device and the heart should play a major role when devising new concepts. Moreover a periodic rotation of the impeller with acceleration and deceleration of the rotor allows for fixed speed while superimposing periodic episodes of pulsatility.

A larger study including more cases may help to better understand the interactions of device-induced flow and native cardiac output and may therefore be of help in optimizing the design of new devices operating with this principle.

Acknowledgements

Fabian Rengier and Matthias Müller-Eschner received support from the German Research Foundation (DFG) within project R03, SFB/TRR 125 "Cognition-Guided Surgery".

Cite this article as: Karmonik C, Partovi S, Rengier F, Meredig H, Farag MB, Müller-Eschner M, Arif R, Popov AF, Kauczor HU, Karck M, Ruhparwar A. Hemodynamic assessment of partial mechanical circulatory support: data derived from computed tomography angiographic images and computational fluid dynamics. Cardiovasc Diagn Ther 2015;5(2):160-165. doi: 10.3978/j.issn.2223-3652.2015.03.03

Disclosure: The authors declare no conflict of interest.

References

1. Meyns B, Ector J, Rega F, et al. First human use of partial left ventricular heart support with the Circulite synergy micro-pump as a bridge to cardiac transplantation. Eur Heart J 2008;29:2582.
2. Meyns BP, Simon A, Klotz S, et al. Clinical benefits of partial circulatory support in New York Heart Association Class IIIB and Early Class IV patients. Eur J Cardiothorac Surg 2011;39:693-8.
3. Barbone A, Pini D, Rega F, et al. Circulatory support in elderly chronic heart failure patients using the CircuLite® Synergy® system. Eur J Cardiothorac Surg 2013;44:207-12; discussion 212.
4. Karmonik C, Partovi S, Loebe M, et al. Influence of LVAD cannula outflow tract location on hemodynamics in the ascending aorta: a patient-specific computational fluid dynamics approach. ASAIO J 2012;58:562-7.
5. Karmonik C, Partovi S, Rengier F, et al. Illustrate flow reversal from retrograde flow pre and post systole to antegrade flow at systole at the origin of the innominate artery and the immediate distal aortic section for case 1. Asvide 2015;2:016. Available online: http://www.asvide.com/articles/470
6. Karmonik C, Partovi S, Rengier F, et al. Show the entire model in similar fashion as supplement #1. Asvide 2015;2:017. Available online: http://www.asvide.com/articles/471
7. Mahmoud M, Kim R, De Luca A, et al. 189 Disturbed flow promotes endothelial cell injury via the induction of developmental genes. Heart 2014;100 Suppl 3:A105.
8. Neth P, Nazari-Jahantigh M, Schober A, et al. MicroRNAs in flow-dependent vascular remodelling. Cardiovasc Res 2013;99:294-303.

